ORIGINAL ARTICLE

Full Factorial Design and Optimization of Olmesartan Medoxomil–Loaded Oily-Core Polymeric Nanocapsules with Improved In-Vitro Stability

Waleed M. Khattab [1] · **Esmat E. Zein El-Dein** [2] · **Sanaa A. El-Gizawy** [2]

Abstract

Purpose This study aims to design oily-core nanocapsules for poorly water-soluble antihypertensive drug olmesartan medoxomil (OM) and optimize systematically the in-vitro characteristics of prepared nanosystems. The study represents an organized methodology for screening and studying significant parameters affecting polymeric nanocapsule formulation and characterization.

Method A full two-level (2^3) factorial design was conducted to optimize the characteristics of poly-Ɛ-caprolactone oily-core nanocapsules (ONC) which were prepared using interfacial deposition of preformed polymer technique. The selected independent variables were the concentration of polymer, aqueous/organic phase ratio, and magnetic stirring rate.

Results The selected formulation and processing variables significantly affected the tested responses. The developed ONC formulae showed a particle size (PS) range from 180.63 ± 0.31 to 338.93 ± 0.42 nm, polydispersity index values (PDI) were < 0.5, negative zeta potential (ZP) values from 20.17 ± 0.21 to 32.83 ± 0.21 mV, and entrapment efficiency (EE) values range from 74.63 ± 0.15 to $93.37 \pm 0.15\%$. In-vitro drug release testing showed a controlled release pattern for OM over 8 h following Hixson-Crowell model for the optimized formula. Transmission electron micrographs (TEM) showed a perfect spherical nanocapsule with a clear polymeric coat. Stability study for 3 months at refrigerated and room temperatures showed non-significant variations and excellent stability for the prepared colloidal nanocapsular dispersion in terms of particle size (PS), zeta potential (ZP), polydispersity index (PDI), and entrapment efficiency (EE).

Conclusion It is concluded that ONC are such a promising nanosystem which can significantly improve the biopharmaceutical behavior of OM.

Keywords Olmesartan · Characterization · Nanoparticles · Polymeric · Nanoprecipitation · Optimization

✉ Waleed M. Khattab
waleedkhattabsu@gmail.com

Esmat E. Zein El-Dein
dr.esmatzein@gmail.com

Sanaa A. El-Gizawy
selgizawy@hotmail.com

[1] Department of Pharmaceutics, College of Pharmacy, Arab Academy for Science, Technology and Maritime Transport, P.O. Box: 1029, Alexandria, Egypt

[2] Department of Pharmaceutical Technology, Faculty of Pharmacy, Tanta University, Tanta, Egypt

Introduction

Olmesartan medoxomil (OM) is an oral antihypertensive medication with a very poor aqueous solubility (less than 7.75 μg/ml). It is classified as a class II drug according to the Biopharmaceutical Classification System (BCS) with a log p value of 2.14 [1]. The absorbed fraction after oral administration is only 0.26 due to poor dissolution and the unabsorbed fraction usually causes gastrointestinal disturbances such as diarrhea, dyspepsia, nausea, vomiting, and abdominal pain [2]. Therapeutic efficacy and tolerability of OM can be controlled by enhancing dissolution which is the rate-limiting step and/or absorption via incorporation into different

nanovesicular structures which can bypass dissolution stage [3].

Nanosizing can be defined as the process of particle size reduction which converts the coarse particles into very minute particles within the nanometer range (1–1000 nm). Nanosizing techniques have become a promising way to enhance the dissolution of poorly water-soluble drugs. Dissolution improvement can be attributed to the increase of total effective surface area which leads to extensive exposure of the particles to the solvent or the surrounding medium. Moreover, the stagnant diffusion layer surrounding any dissolving particle is usually reduced in thickness which increases the concentration gradient leading to more and rapid dissolution. Class II BCS drugs are usually suffering from poor bioavailability due to the limited dissolution rather than GI penetration capability. Therefore, dissolution enhancement is the shortest way to promote absorption and improve absolute oral bioavailability [4].

Nanocapsules, which are a characteristic class of nanoparticles, are usually composed of an oily or aqueous core containing one or more active materials and a protective shell [5] in which the therapeutic substance may be incorporated. Nanocapsules have attracted a great interest in biomedical field because of their protective coating and controlled release characteristics [6]. Interfacial deposition of preformed polymer technique can be considered as a simple and reproducible method for preparation of nanocapsules. It is based on employing two phases which are solvent and non-solvent phase [7]. Solvent phase is usually composed of an organic solvent such as acetone, oil, polymer as a film former, w/o surfactant and the active substance. Non-solvent phase is usually aqueous one containing a stabilizing agent such as Tween 80. The organic phase is injected inside the aqueous phase with a constant injection rate during magnetic stirring until the formation of opalescent colloidal dispersion of nanocapsules; then, the organic solvent is removed using rotary evaporation technique under reduced pressure.

Characteristics of the prepared nanocapsules such as particle size (PS), polydispersity index (PDI), and zeta potential (ZP) depend mainly on type and concentration of polymer, aqueous/organic phase ratio, and fluid dynamics or magnetic stirring rate [7]. Poly-Ɛ-caprolactone is a US Food and Drug Administration (FDA)-approved biodegradable semi-crystalline aliphatic polyester which can be used for controlled delivery of medicaments and has high permeability to drugs [8]. Various oils can be used for production of oily-core nanocapsules (ONC) but caprylic/capric triglyceride types are often used because of their wide range of solubility for active substances [7]. The most commonly used w/o surfactants are sorbitan esters and phospholipids [7]. Acetone is mostly the organic solvent of choice.

Colloidal nanocapsular dispersions are considered as stable systems due to Brownian motion, but their stability may be disrupted due to polymer degradation, migration of the active substance out of the core, and microbiological contamination of aqueous medium.

Design of experiments (DOE) is used as a testing tool to view the impact of large number of process and formulation variables associated with pharmaceutical formula development [9]. Factorial design particularly is the most widely used method in optimization of pharmaceutical formulae as it produces polynomial mathematical relationships facilitating the selection of optimal parameters [10].

Several trials were conducted for preparation of OM-loaded nanosystems such as self-nanoemulsifying drug delivery system (SNEDDS) [11], nanostructured lipid carriers (NLC) [12] and nanosuspension [13].

Oily-core nanocapsules for OM are still not fully studied or optimized with respect to the in-vitro characteristics and stability. Furthermore, a factorial design study was not previously conducted to show effect of different variables on the properties of ONC prepared using nanoprecipitation.

The aim of the present study is to formulate oily-core poly-Ɛ-caprolactone nanocapsules of OM via nanoprecipitation technique based on a factorial design to optimize the in-vitro characteristics for the prepared nanocapsules then evaluate the stability of the produced colloidal nanocapsular dispersion.

Materials and Methods

Materials

Olmesartan medoxomil (Jedco International Pharmaceuticals, Cairo, Egypt), Labrafac PG (Gattefossé, Saint-Priest, France), poly-Ɛ-caprolactone (PCL, Mw = 14 kDa, Sigma-Aldrich, Japan), Span 40 and 60 (Alpha Chemika, Mumbai, India), Tween 80, acetone, methanol, mannitol, potassium dihydrogen orthophosphate, disodium hydrogen phosphate, potassium chloride, sodium chloride, sodium hydroxide (El-Gomhouria Pharmaceuticals, Cairo, Egypt). All chemicals and reagents used were of analytical grade. They have been reported by their manufacturers as providing best results for their uses. Demineralized and double distilled water was used throughout the experiments.

Methods

Preliminary Trials for Preparation of OM-ONC

OM-ONC were prepared using nanoprecipitation technique as described by Mora-Huertas et al. [7]. Initially, seven formulae (FI–FVII) were developed to check for variations in PS, ZP, and PDI and selection of three variables to be employed in a factorial design at two levels. The suggested formulation and

processing variables were concentration of polymer, concentration and type of w/o surfactant, concentration of stabilizer, aqueous/organic phase ratio, organic phase injection rate, and magnetic stirring rate. The proposed OM-ONC composition is shown in Table 1. First, organic phase was prepared by dissolving OM, Span 40 or 60, PCL and Labrafac in acetone using magnetic stirring and gentle warming at 40 °C for 15 min to ensure complete dissolution. Second, aqueous phase was prepared by dissolving Tween 80 in double distilled water. Organic phase is then slowly injected into aqueous phase using syringe pump (Phoenix, France) at different injection rates under continuous stirring till formation of milky white opalescent colloidal dispersion. Third, all formulae were concentrated by removal of the organic solvent and part of water using a rotary evaporator (Heidolph, vv2000, Germany) at 130 rpm and 40 °C for 15–20 min until the final volume reached 15 ml and then stored in a refrigerator at 4 °C.

Experimental Factorial Design

A three-factor, two-level (2^3) randomized full factorial design was applied in the present study to optimize the OM-ONC. The selected independent variables were concentration of PCL (factor A) at two levels (0.5 and 0.8% w/v), aqueous/organic phase ratio (factor B) at two levels (1.8:1 and 2.3:1), and magnetic stirring rate (factor C) at two levels (300 and 800 rpm). The tested responses were PS, ZP, PDI, and EE. The experimental trials were performed at all eight possible combinations. OM-ONC were prepared according to the composition shown in Table 2 by the same nanoprecipitation technique which was employed for the preliminary trials.

Table 2 Proposed composition of the prepared OM-ONC formulae

Experimental design

Ingredients/formulae	F1	F2	F3	F4	F5	F6	F7	F8
OM (mg)	20	20	20	20	20	20	20	20
PCL (mg)	75	125	75	125	75	125	75	125
Labrafac PG (µl)	150	150	150	150	150	150	150	150
Span 60 (mg)	100	100	100	100	100	100	100	100
Acetone (ml)	30	30	30	30	30	30	30	30
Tween 80 (µl)	200	200	200	200	200	200	200	200
Water (ml)	55	55	70	70	55	55	70	70
Final volume (ml)	15	15	15	15	15	15	15	15

Characterization of Prepared OM-ONC

Particle Size and Polydispersity Index Analysis

PS and PDI of all formulae were measured using dynamic light scattering technique of Malvern Zetasizer (MZ) (Malvern Instruments Ltd., UK, equipped with Malvern PCS software version 6.20). Prior to each measurement, 20 µl from each formula was diluted with double distilled water (DDW) up to 10 ml (500× dilutions). Light scattering was monitored at 25 °C at a scattering angle of 90°. All measurements were performed in triplicates and the mean ± SD was calculated.

Zeta potential Measurement

ZP was determined using MZ. Samples from each formula were transferred into a folded capillary cell equipped with platinum electrode. Dispersion technology software built into

Table 1 Proposed formula composition and processing parameters for preliminary studies to prepare OM-ONC

Preliminary experimental design

	Ingredients/formulae/parameters	FI	FII	FIII	FIV	FV	FVI	FVII
Organic phase	OM (mg)	20	20	20	20	20	20	20
	PCL (mg)	100	100	150	200	100	100	100
	Labrafac PG (µl)	150	150	150	150	150	150	150
	Span 40 (mg)	–	–	–	–	–	50	–
	Span 60 (mg)	50	50	50	50	100	–	50
	Acetone (ml)	30	30	30	30	30	30	30
Aqueous phase	Tween 80 (µl)	150	150	150	150	200	150	150
	Water (ml)	55	55	55	55	70	55	55
Processing parameters	Injection rate (ml/h)	80	100	80	100	100	100	Pouring
	Dynamics/stirring rate (rpm)	300	300	500	800	800	300	300
	Temperature during process (°C)	40	40	40	40	40	40	40
	Rotary evaporation	130 rpm at 40 °C for 15–20 min						
	Final volume (ml)	15	15	15	15	15	15	15

the MZ was used for ZP values' calculation. All measurements were performed at 25 °C in triplicates and the mean ± SD was calculated.

Drug Entrapment Efficiency Measurement

Entrapment efficiency (EE) was determined by indirect method. Concentration of free drug was first determined then subtracted from the theoretical total drug concentration (1.33 mg/ml) to calculate the concentration of entrapped drug which was then divided by the total drug concentration. EE was calculated and expressed as a percentage.

OM-ONC formulae (2 ml) were centrifuged at 15,000 rpm for 1 h at 4 °C using a cooling centrifuge. The supernatant was filtered immediately using 0.1-µm PTFE syringe filter (Whatman Inc., Clifton, NJ, USA) to ensure that all nanocapsules were separated. Then, it was diluted appropriately using methanol, measured spectrophotometrically at maximum wavelength 256 nm employing UV-Vis spectrophotometer (Pg 80+, Pg instruments, UK), and the free drug concentration was calculated from the calibration plot. All measurements were performed in triplicates and the mean ± SD was calculated.

In-Vitro Release Study of OM from Prepared ONC

OM release from ONC was evaluated using dialysis bag method [10]. The objective of this study is to test the drug release behavior from the core of prepared nanocapsules. However, the dialysis membrane may hinder the drug diffusion as well as there is little agitation inside the bag. Therefore, sink condition is not applicable here [14].

Each OM-ONC formula (1 ml) containing 1.33 mg OM approximately was sealed in a cellulosic dialysis membrane (SERVAPOR dialysis tubing, cutoff 12–14 KDa, Serva, Heidelberg, Germany) and then it was immersed into a beaker containing 50 ml of phosphate buffer saline PBS (pH 7.4) [2]. The entire system was placed over magnetic stirrer and kept under continuous stirring at 250 rpm for just 8 h since sink condition is not present. The temperature was maintained at 37 ± 0.5 °C. Samples from the receiving medium (3 ml) were collected and replaced with the same volume of fresh medium at predetermined time intervals. The collected samples were then measured spectrophotometrically at maximum wavelength 257 nm. All measurements were performed in triplicates and the mean ± SD was calculated.

Kinetic Treatment for the In-Vitro Release of OM from Prepared OM-ONC

Release kinetic modeling was employed for evaluation of invitro release of OM from different OM-ONC formulae. Furthermore, the in-vitro release and its kinetic treatment can be used to predict the way by which the drug may perform inside the body. The in-vitro release data were subjected to analysis process using different kinetic models including zero order, first order, Higuchi, Hixson-Crowell models, and Baker-Lonsdale equation [15].

$$\text{Zero−order kinetics}: Q_t = kt \tag{1}$$

$$\text{First−order kinetics}: ln\,(Q_0{-}Q_t) = -kt + Q_0 \tag{2}$$

$$\text{Higuchi model}: Q_t = kt^{1/2} \tag{3}$$

$$\text{Hixson − Crowell model}: (1 - Q_t)^{1/3} = 1{-}\,kt \tag{4}$$

$$\text{Baker − Lonsdale equation}: 3/2 \left[1 - (1 - Q_t)^{2/3}\right] - Q_t = kt \tag{5}$$

where Q_0 is the initial quantity of drug, Q_t is the quantity of drug released after time (t), and k is the reaction rate constant.

For all prepared OM formulae, three parameters were calculated in the applied orders and models. These parameters were correlation coefficient (R^2), reaction rate constant (K), and half-life (T_{50}).

Statistical Analysis

Statistical analysis for the predetermined parameters in the present study was performed using Minitab statistical software. The factorial design was statistically analyzed by multiple regression analysis. A statistical model incorporating interactive and polynomial terms was used to evaluate the response as described by the following equation:

$$Y = b_0 + b_1\text{A} + b_2\text{B} + b_3\text{C} + b_{12}\text{AB} + b_{13}\text{AC}$$
$$+ b_{23}\text{BC} + b_{123}\text{ABC} \tag{6}$$

where Y is the dependent variable, b_0 is the arithmetic mean response of the eight runs, and b_i is the estimated coefficient for the factor i. The mean effect (A, B, and C) represents the average result of changing one factor at a time from its low to high level. The interaction terms (AB, AC, BC, and ABC) show how the response changes when two factors are changed simultaneously. The significance, validation of the chosen model, and the contribution of each factor with different levels on response were evaluated by two-way analysis of variance (ANOVA) at 95% significance level ($p < 0.05$).

Optimization of Prepared OM-ONC

All regression analyses which were performed using design of experiment (DOE) feature in Minitab software were employed to optimize the results of the measured responses and to find the optimum formula for further investigation using response optimizer.

Morphology Assessment of OM-ONC Using Transmission Electron Microscopy

The morphology and size of the prepared OM-ONC optimum formula were observed using a transmission electron microscope (JEM-2100, Pleasanton, CA, USA). Prior to imaging, the OM-ONC samples were diluted 100 times with double distilled water. A drop from the formula was deposited on a film-coated copper grid forming a thin liquid film. The films were then negatively stained with 2% (w/v) phosphotungstic acid solution. After air drying, the stained films were photographed by TEM [16].

Thermal Analysis

The objective of this study is to detect changes in drug crystallinity after being encapsulated inside the oily-core nanocapsules. Powder samples of pure OM, PCL, mannitol (cryoprotectant), and freeze-dried-optimized OM-ONC were subjected to thermal analysis using differential scanning calorimeter (DSC equipment, Perkin Elmer DSC-6, USA) after calibration with indium. The samples were heated and dried under nitrogen gas. The heating range of the process was 20–400 °C and the rate of temperature rise was 10 °C/min.

Powder X-Ray Diffraction

This study aims to monitor the crystalline structure of OM before and after encapsulation inside the oily-core nanocapsules. Powder samples of pure OM and freeze-dried-optimized OM-ONC were analyzed using X-ray diffractometer (GNR APD 2000, Novara, Italy). This equipment utilizes Cu Kα radiation (1.54056 Å) and it is supported with a Gobel mirror. Diffraction pattern is detected via a SuperSpeed VANTEC-1 detector. The procedures were carried out at ambient temperature employing continuous scan mode with 2theta scan axis. The data was collected in the range of (4–60°) and a scanning step size of 0.03°.

Stability Study

Optimized formula of OM-ONC was stored at room temperature and refrigerated temperature [17] for 3 months. PS, PDI, ZP, and EE were measured monthly as described before to monitor any significant changes during storage.

Results and Discussion

Preliminary Trials for Preparation of OM-ONC

Preliminary developed OM-ONC formulae showed promising results in terms of PS, PDI, and ZP.

PS of nanoparticles is an important determinant of its physicochemical properties and physiological performance [18]. Generally, the average PS of polymeric nanoparticles ranges from 100 up to 500 nm [7]. However, PS of nanoparticles which are prepared via nanoprecipitation technique is usually between 150 and 500 nm [19].

Different preliminary formulae (FI–FVII) showed particle size range from 251.2 ± 2.0 to 397.5 ± 1.1 nm. Smallest PS was recorded for formula (FV) when PCL was added in a concentration of 0.7% w/v, span 60 was also incorporated to the formula in a concentration of 0.7% w/v, Tween 80 was used as a stabilizer in a concentration of 1.3% v/v, aqueous/organic phase ratio was 2.3:1, organic phase injection rate was 100 ml/h, and magnetic stirring rate was 800 rpm. When PCL concentration was increased to 1.3% w/v, OM-ONC showed larger PS which may be due to increase in the polymeric coat thickness around the nanocapsules even if the stirring rate was increased. These results may also be attributed to the fact that increasing polymer concentration can affect organic phase viscosity which reduces the diffusion of organic phase into aqueous phase and reduces the efficiency of stirring leading to larger nanocapsules [20]. These results are in compliance with the results of Rodriguez et al. [21] who prepared nanoparticles using Eudragit L100-55 via nanoprecipitation method to study effect of polymer concentration on PS using different organic solvents and found that increasing polymer concentration in organic phase led to large PS.

Decreasing PCL concentration to 0.7% w/v or 1% w/v led to smaller PS depending on the magnetic stirring rate. PS was found to be 397.5 ± 1.1 nm when PCL concentration was 1.33% w/v at a magnetic stirring rate 800 rpm. PS was reduced to 251.2 ± 2.0 nm when PCL concentration was 0.7% w/v using the same magnetic stirring rate (800 rpm). However, when PCL concentration was 0.7% w/v with a magnetic stirring rate 300 rpm, PS was found to be 368.1 ± 3.1 nm.

Generally, high magnetic stirring rates up to 800 rpm led to smaller PS which may be due to rapid formation of nanocapsules with high disturbance in the medium which prevented the aggregation of the particles. High magnetic stirring rate may also lead to more efficient shear mixing and rapid diffusion of organic phase through the aqueous phase. These results are in compliance with Asadi et al. [22], who reported that increasing stirring rate will lead to smaller particles.

Aqueous/organic phase ratio showed a significant effect on PS. PS of prepared nanocapsules was reduced from 340.8 ± 1.5 to 251.2 ± 2.0 nm by increasing aqueous/organic phase ratio from 1.8:1 to 2.3:1. This may be attributed to rapid diffusion of organic phase through the aqueous phase and better dispersion of formed nanocapsules without aggregation.

PDI values for all formulae were in the range of 0.2–0.4 which shows uniformity in PS distribution across the colloidal dispersion and minimum variations. This may be attributed to

the use of acetone as an organic solvent which is miscible with water and has a high diffusion rate which allows uniform formation of nanocapsules.

Zeta potential (ζ) is the measure of electrokinetic potential and is the only accessible tool to characterize the double-layer properties of the colloidal systems. This potential provides a realistic magnitude of surface charge on the colloids [23]. The colloidal dispersion shows acceptable physical stability if the zeta potential of the particles is less than -15 mV or more than $+15$ mV [24].

All formulae showed negative ZP values which are attributed to ionized carboxylic groups of PCL in aqueous medium. ZP values were in the range of -22.5 ± 0.7 to -34.1 ± 0.5 mV which indicates good stability for the nanosystem.

Depending on these preliminary trials, it was concluded that the three variables which were significant on characteristics of prepared OM-ONC are polymer (PCL) concentration, aqueous/organic phase ratio, and magnetic stirring rate. These variables were added to the selected factorial design to prepare eight different formulae (F1–F8).

Characterization of Prepared OM-ONC

PS and PDI

Particle size and size distribution plays a critical role in nanocapsule system since it affects the in-vivo distribution, bioavailability, toxicity, the capacity of drug loading, drug release, and the stability of nanoparticulate systems [25]. Table 3 summarizes the average PS in nanometric range and PDI values of different OM-ONC formulae. PS of tested nanocapsules ranged from 180.63 (F7) to 338.93 nm (F3). All PDI values were less than 0.5. A representative chromatogram for F1 particle size distribution is shown in Fig. 1a.

Stepwise multivariate linear regressions were performed to evaluate the relationship between the response Y1 (nanocapsule PS) and the independent variables (A, B, C, AB, AC, BC, ABC) as reported in Eq. (7):

$$PS = 254.083 - 10.5917\,A - 0.9000\,B - 35.1083\,C$$
$$+ 3.9917\,AB$$
$$+ 11.2833\,AC - 33.4917\,BC - 0.7333\,ABC \quad (7)$$

Regression analysis revealed the significant effect of all tested factors and interactions ($p < 0.05$) on PS. The most effective factor was C (magnetic stirring rate) with a negative coefficient value indicating that the use of high stirring rates (800 rpm) during nanoprecipitation technique of nanocapsule formulation significantly results in PS reduction. The interaction BC (interaction of aqueous/organic phase ratio and stirring rate) was found that it can significantly affect PS of nanocapsules with a negative coefficient value which means that high aqueous/organic phase ratio (2.3:1) and stirring rate (800 rpm) favor the production of smaller nanocapsule PS as in F7 and F8. Moreover, the results showed that the impact of factor A (PCL concentration) is more significant than factor B (aqueous/organic phase ration) on PS. Concerning the use of high stirring rates in nanoprecipitation technique, PS reduction may be attributed to enhanced mass transfer and high diffusion rate leading to prompt nucleation and precipitation. However, Huang and Zhang who studied the effect of different stirring rates (0, 125, 350, 700, 1100, 1200) on nanoparticle size reported that this factor is insignificant [26].

The effect of the independent variables on PS is demonstrated graphically using the generated response surface and contour plots in Fig. 2.

Stepwise multivariate linear regressions equation for the response Y2 (PDI) is as follows:

$$PDI = 0.300125 - 0.016458\,A$$
$$+ 0.001375\,B - 0.047792\,C + 0.007458\,AB$$
$$+ 0.009458\,AC - 0.051875\,BC + 0.001042\,ABC \quad (8)$$

Table 3 Characterization of OM-ONC formulae fabricated via 2^3 full factorial design

Formula	Characteristics[a]			
	Particle size (nm)	Polydispersity index	Zeta potential (mV)	Entrapment efficiency (%)
F1	$283.20 \pm (0.62)$	$0.33 \pm (0.002)$	$-20.77 \pm (0.12)$	$93.37 \pm (0.15)$
F2	$230.00 \pm (0.44)$	$0.26 \pm (0.002)$	$-26.27 \pm (0.15)$	$89.07 \pm (0.12)$
F3	$338.93 \pm (0.42)$	$0.42 \pm (0.002)$	$-29.53 \pm (0.06)$	$86.23 \pm (0.12)$
F4	$304.63 \pm (0.55)$	$0.38 \pm (0.002)$	$-29.27 \pm (0.21)$	$85.47 \pm (0.06)$
F5	$255.93 \pm (0.45)$	$0.32 \pm (0.002)$	$-32.83 \pm (0.21)$	$76.00 \pm (0.10)$
F6	$250.80 \pm (0.46)$	$0.29 \pm (0.003)$	$-27.00 \pm (0.10)$	$74.63 \pm (0.15)$
F7	$180.63 \pm (0.31)$	$0.20 \pm (0.003)$	$-30.67 \pm (0.21)$	$77.13 \pm (0.12)$
F8	$188.53 \pm (0.25)$	$0.20 \pm (0.002)$	$-20.17 \pm (0.21)$	$79.30 \pm (0.10)$

[a] Values are expressed as mean $\pm$ SD ($n = 3$)

Fig. 1 **a** A representative chromatogram showing particle size distribution of OM-ONC (F1). **b** ZP analysis chart for OM-ONC (F1)
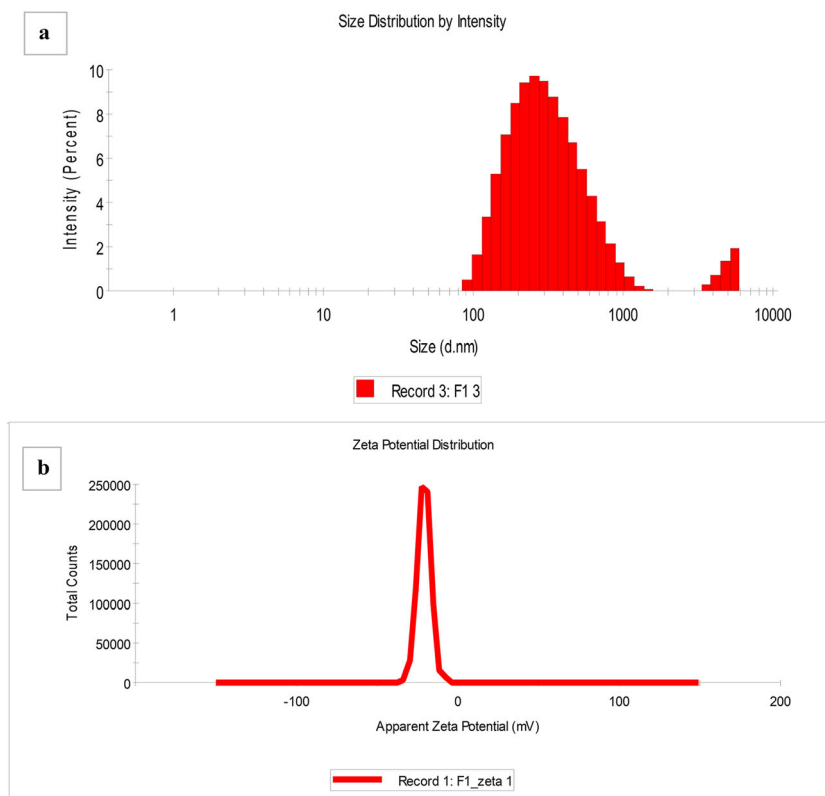
Regression analysis revealed that none of the tested variables significantly affected PDI values. This result may be due to the fact that nanoprecipitation technique is not including homogenization or sonication process which is usually employed in other methodologies.

However, interaction BC (interaction of aqueous/organic phase ratio and stirring rate) may be the most effective factor on PDI values with a negative coefficient value indicating that the use of high aqueous/organic phase ratio (2.3:1) and stirring rate (800 rpm) may enhance the uniformity in PS distribution of the colloidal dispersion as in F7 and F8 which may be attributed to high diffusion rate of organic phase through aqueous phase during the nanoprecipitation technique as mentioned before.

The effect of the independent variables on PDI is demonstrated graphically using the generated response surface and contour plots in Fig. 3.

ZP Measurement

Table 3 summarizes the average ZP values for every OM-ONC formula. ZP values of prepared OM-ONC ranged from -20.17 (F8) to -32.83 mV (F5). A representative ZP analysis chart of F1 is shown in Fig. 1b.

Stepwise multivariate linear regressions were performed to evaluate the relationship between the response Y3 (ZP) and

the independent variables (A, B, C, AB, AC, BC, ABC) as reported in Eq. (9):

$$ZP = 27.0625 - 1.3875\,A + 0.3458\,B$$
$$+ 0.6042\,C - 1.3042\,AB - 2.6958\,AC - 2.5958\,BC$$
$$+ 0.1375\,ABC \tag{9}$$

Regression analysis revealed the significant effect of all tested factors and interactions ($p < 0.05$) on the ZP values. The effect of the independent variables on ZP is demonstrated graphically using the generated response surface and contour plots in Fig. 4. The most effective factor was AC (interaction between PCL concentration and magnetic stirring rate) with a negative coefficient value indicating that high concentration of PCL and stirring rate will result in less ZP values (more negative) which is attributed to the fact that PCL has ionized carboxylic groups in aqueous medium, as previously mentioned. High concentration of PCL can lead to a thick polymeric coat layer with high density of surface negative charges. This change in ZP values can be attributed to the shielding effect by the stabilizer molecules (Tween 80) at the interface due to interaction with PCL. Therefore, high polymer concentration with a constant stabilizer concentration and high stirring rate can decrease the number of Tween 80 molecules available at the interface resulting in a reduced shielding effect and more negative ZP values [27]. These results are in
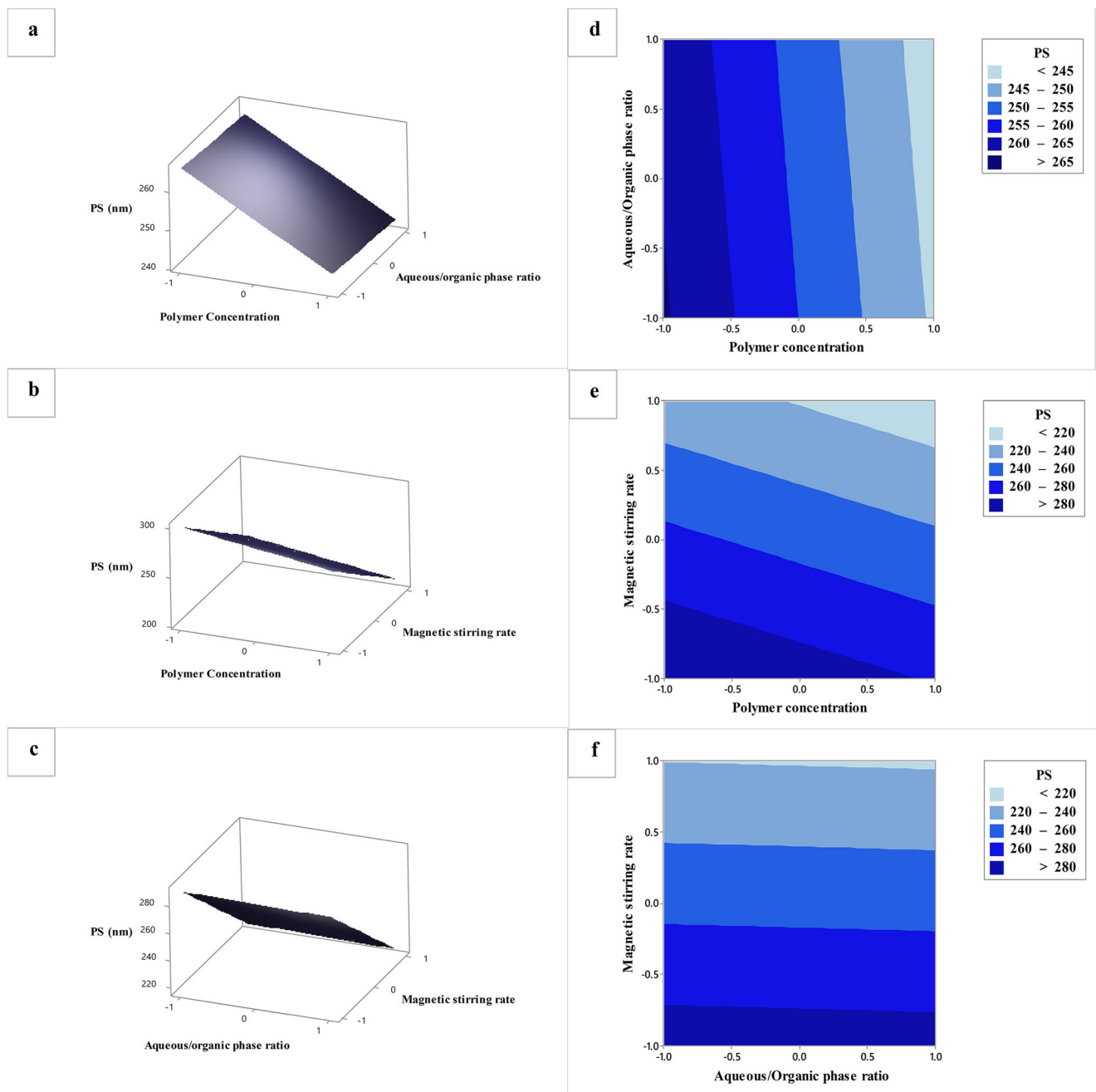
Fig. 2 Response surface (a, b, c) and contour plots (d, e, f) showing effect of independent variables on PS

agreement with those reported previously by Ajiboye et al. [28] who formulated PCL nanoparticles and used different concentrations of PCL to study the effect of different concentrations on surface charge of the particles. This research showed that increasing PCL concentration led to more negative ZP values.

Entrapment Efficiency

EE was calculated based on the calibration plot in methanol (concentration range 2.5–35 µg/ml, y = 0.0439x + 0.003,

$R^2 = 0.9997$). Table 3 summarizes the average EE values for every OM-ONC formula. EE values of prepared OM-ONC ranged from 74.63 (F6) to 93.37% (F1).

Stepwise multivariate linear regressions were performed to evaluate the relationship between the response Y4 (EE) and the independent variables (A, B, C, AB, AC, BC, ABC) as reported in Eq. (10):

$$EE = 82.6500 - 0.5333\,A - 0.6167\,B - 5.8833\,C$$
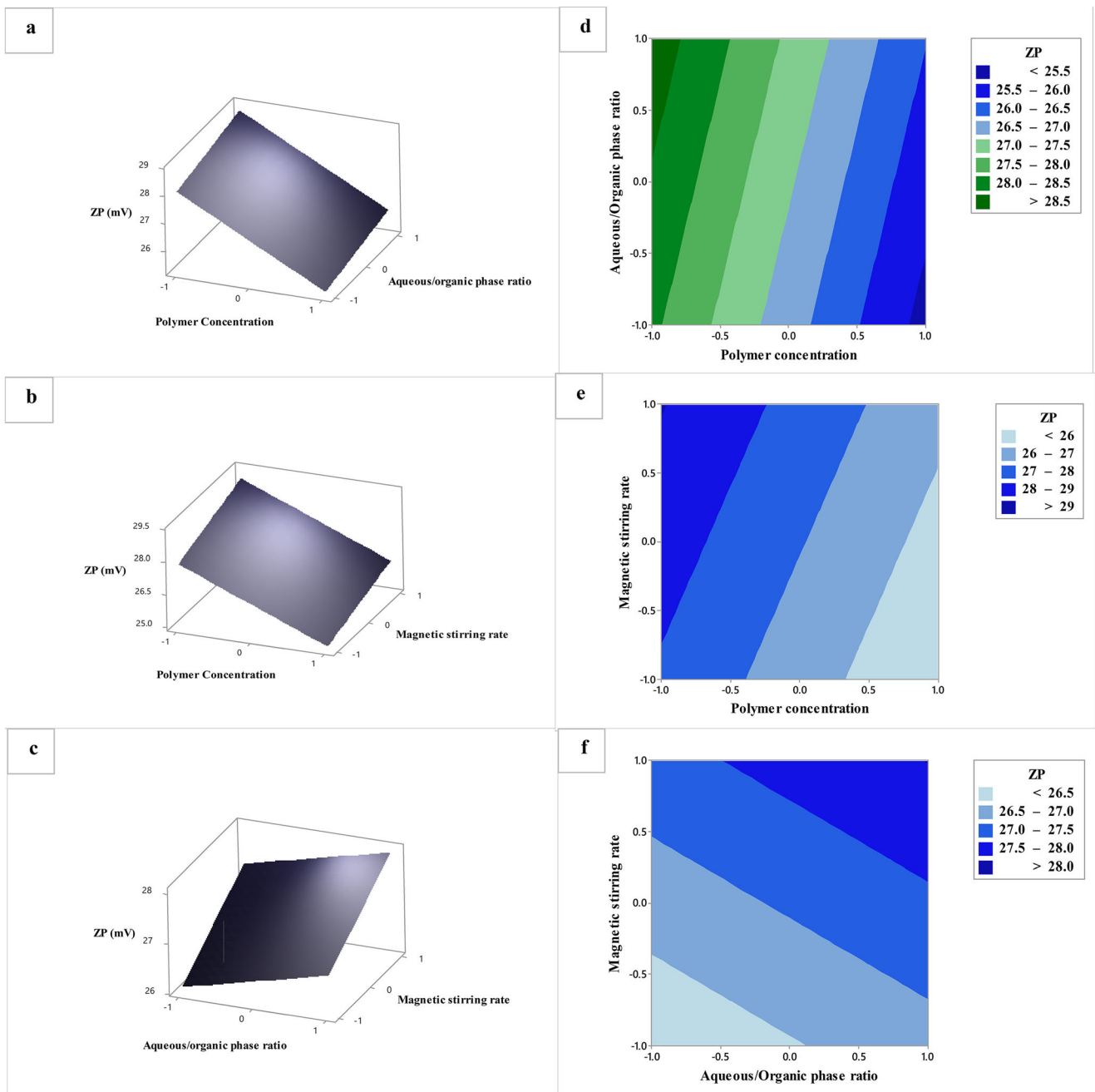
$$+ 0.8833\,AB + 0.7333\,AC + 2.0667\,BC \qquad (10)$$
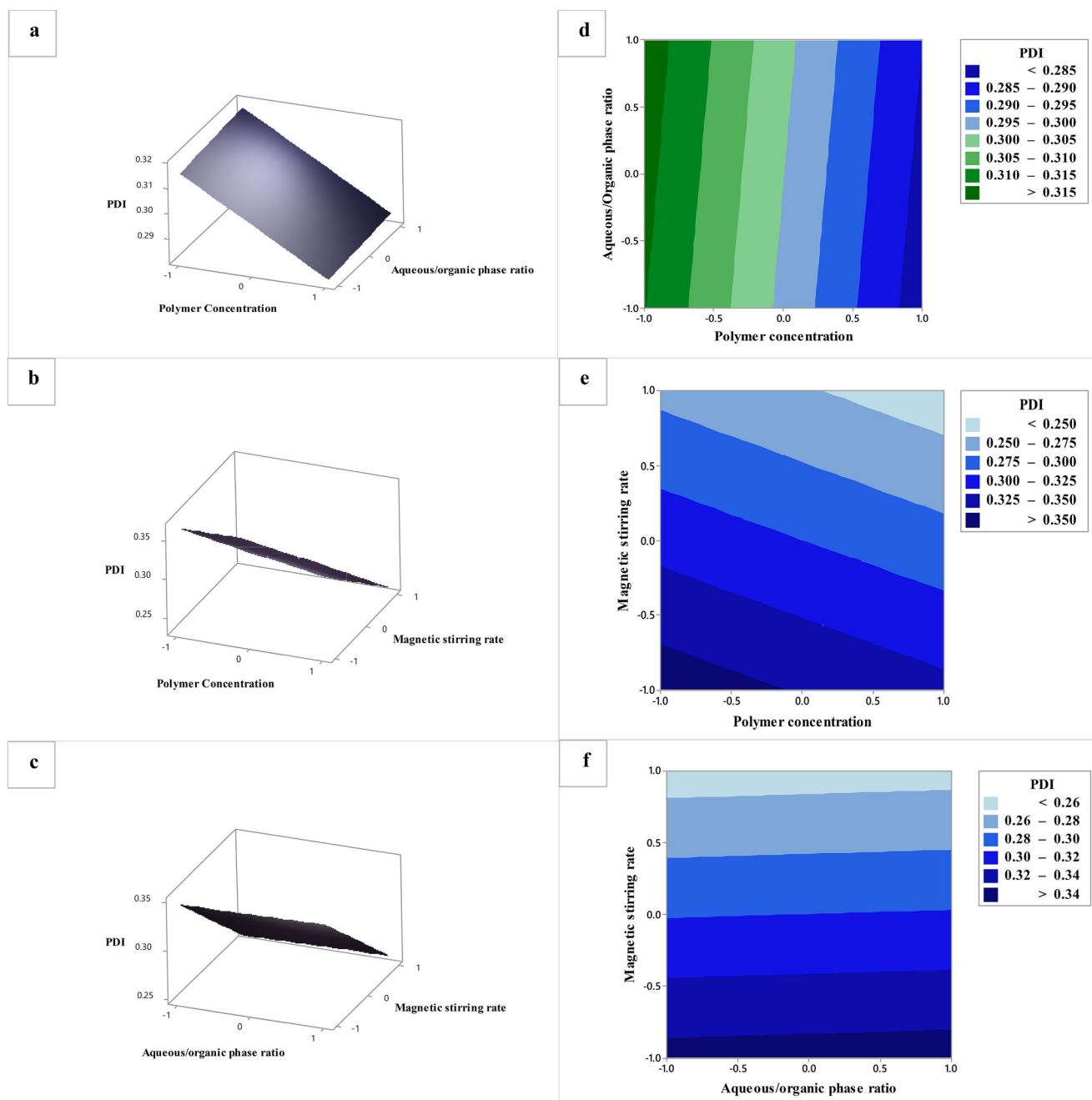
Fig. 3 Response surface (**a**, **b**, **c**) and contour plots (**d**, **e**, **f**) showing effect of independent variables on PDI

Regression analysis revealed the significant effect of all tested factors and interactions ($p < 0.05$) on the EE values (except the interaction ABC). The effect of the independent variables on EE is demonstrated graphically using the generated response surface and contour plots in Fig. 5. The most effective factor was C (magnetic stirring rate) with a negative coefficient value indicating that high stirring rate (800 rpm) significantly reduces entrapment of the drug (OM) inside the ONC which is related to the effect of the stirring rate on the PS. Small-sized ONC may lack the high EE values due to the limited space of the oily-core. High stirring rate may also lead to a certain degree of porosity on the polymeric coat of the prepared ONC which could result in leakage of the loaded drug out of the nanocapsule after its formation at the end of the nanoprecipitation technique. These results contradict the findings reported by Awotwe-Otoo et al. [29] who formulated anti-cancer drug-loaded PLGA nanoparticles using emulsification-solvent evaporation technique at two different

Fig. 4 Response surface (**a**, **b**, **c**) and contour plots (**d**, **e**, **f**) showing effect of independent variables on ZP

stirring rates (600, 1200 rpm) and concluded that the stirring rate effect on EE is statistically non-significant.

In-Vitro Release Study of OM from Prepared ONC

All OM-ONC showed a drug release and diffusion across the dialyzing membrane. The release pattern was different among formulae. The cumulative percentage drug released after 8 h was calculated based on the calibration plot in PBS (concentration range 1.5–40 µg/ml, $y = 0.0294x + 0.0448$, $R^2 = 0.9997$). The results ranged from $41.7 \pm 2.8\%$ (F8) to $93.9 \pm 3.9\%$ (F2) while the pure drug suspension in double distilled water showed a release of $25.6 \pm 1.97\%$ after 8 h.

Release profiles of OM-ONC are shown in Fig. 6a. Generally, poor aqueous solubility of OM may be the reason for the slow release pattern of the drug from the lipophilic core of nanocapsules since the drug is only present inside the core and not in the outer polymeric coat. However, the results of this study showed that the highest percentage release of the drug was from the nanocapsule colloidal dispersion (F1 and F2) prepared
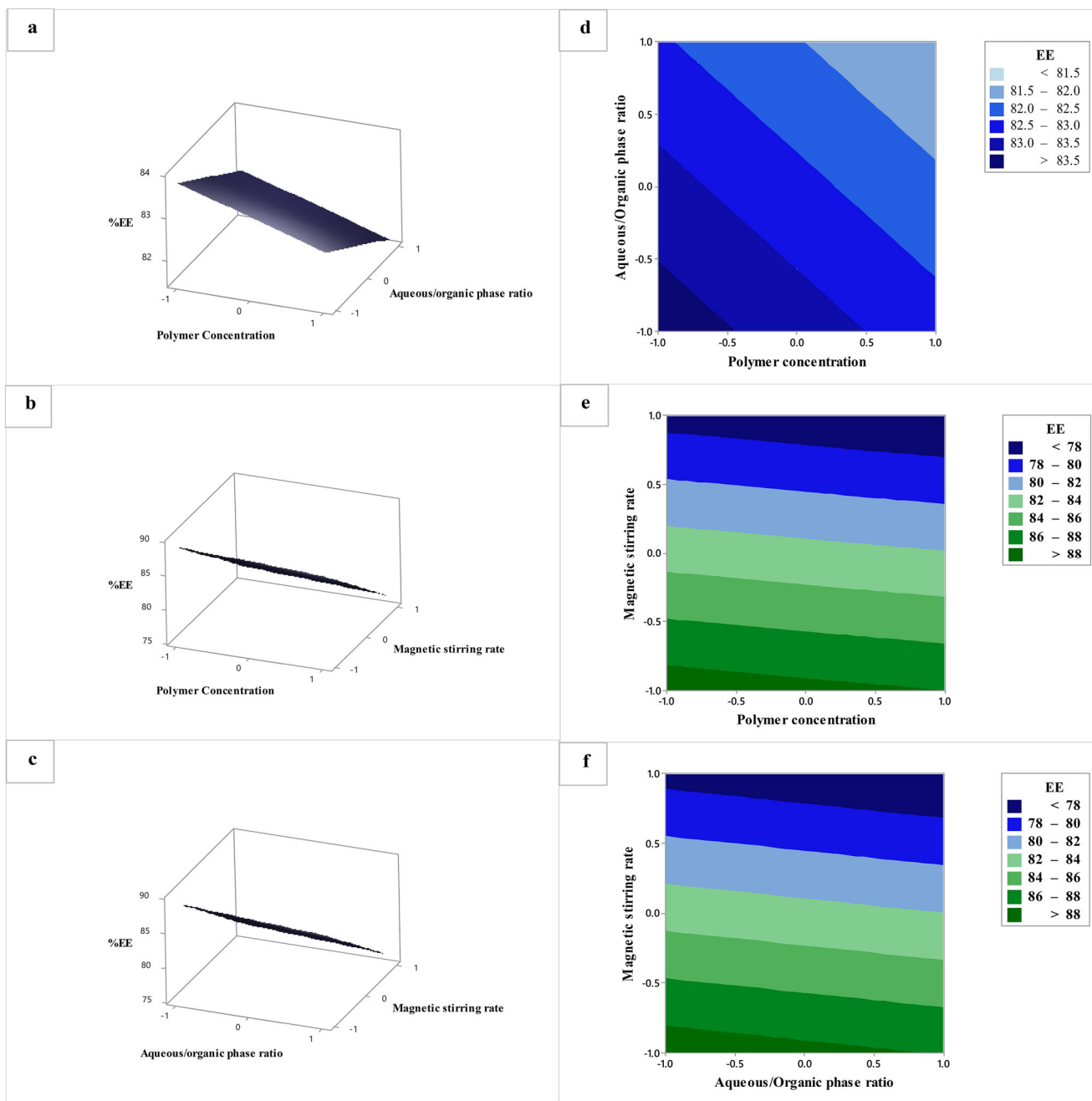
Fig. 5 Response surface (**a**, **b**, **c**) and contour plots (**d**, **e**, **f**) showing effect of independent variables on EE

using low aqueous/organic phase ratio (1.8:1) and low stirring rate (300 rpm).

OM-ONC release profiles were higher than the release profile of pure drug suspension since the nanosizing process led to enhanced dissolution and the crystallinity of the drug was changed after encapsulation.

The release kinetics of OM from ONC were analyzed by fitting the in-vitro release data to different mathematical kinetic models. The correlation coefficients were compared, and the release kinetic parameters are reported in Table 4.

Optimization of the Prepared OM-ONC

Response optimization was carried out on different formulae based on the four measured responses (PS, PDI, ZP, and EE). The suggested optimization process was based on the selection criteria for the optimum formula which includes selection of PS with a target value 300 nm, PDI with a target value 0.25, ZP with a target value − 25 mV, and maximizing the value for EE since it has a high impact on the major objective of the study which is related to enhancing the oral bioavailability of OM via nanoencapsulation inside the oily-core of polymeric

Fig. 6 a In-vitro release profile of OM from different ONC formulae in PBS pH 7.4 at 37 °C (mean ± SD, $n = 3$). **b** TEM micrograph of prepared nanocapsules showing a clear polymeric coat. **c** TEM micrograph of a sample from the nanocapsule dispersion showing uniform and small size particles < 100 nm
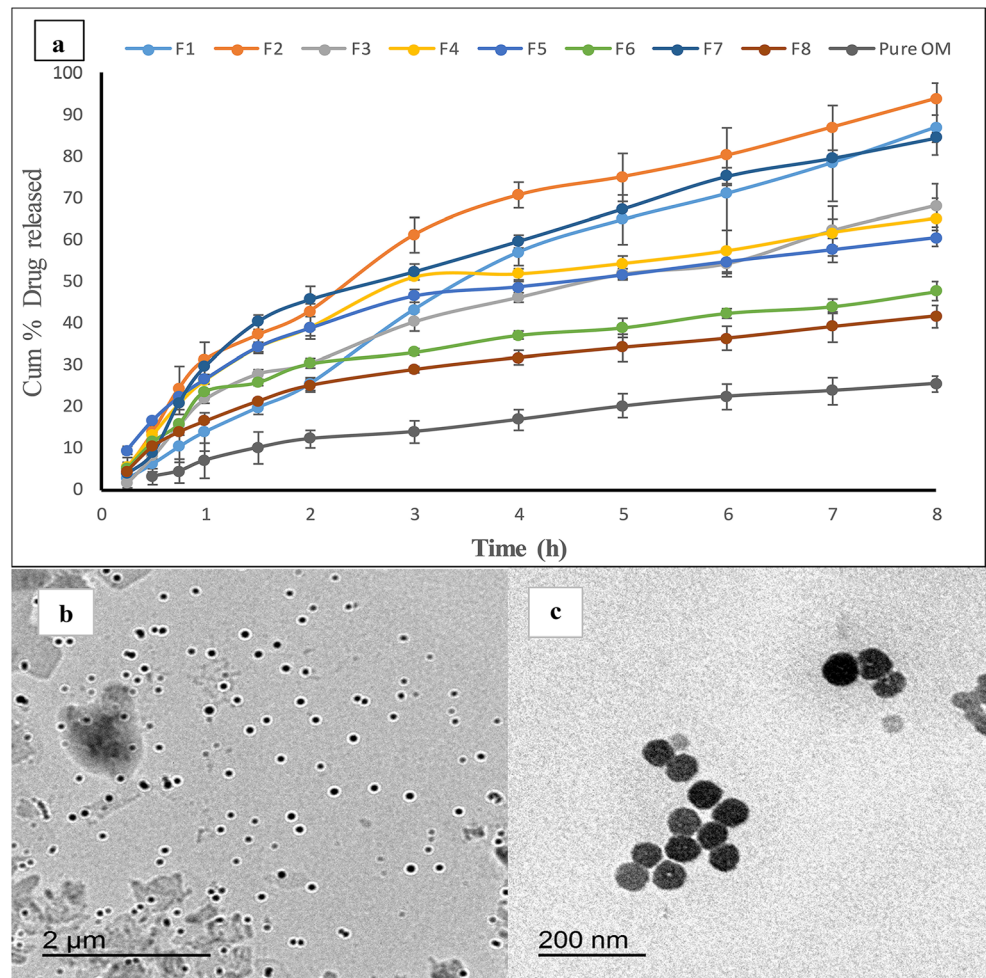
nanoparticles to promote dissolution process which is considered the rate-limiting step for absorption of class II BCS drugs.

According to the optimization plot (shown in Fig. 7) generated via Minitab software, the optimum formula selected is the one prepared using a polymer concentration of 0.5% w/v, aqueous/organic phase ratio 1.8:1, and magnetic stirring rate 300 rpm (F1) with a desirability factor 0.812.

Morphology Assessment of OM-ONC Using Transmission Electron Microscopy

TEM micrographs of optimum formula F1 as shown in Fig. 6b and c revealed that the OM-ONC were formed properly in a uniform spherical shape via the nanoprecipitation technique with a clear polymeric coat (the transparent region

Table 4 In-vitro release kinetic parameters for OM-ONC formulae in PBS (pH 7.4)[a]

Formula	Best fit mathematical model	Correlation (R^2)	T_{50} (h)	Rate constant (K)	Cumulative % drug released after 8 h
F1	Hixson-Crowell	0.998	3.37	0.28	86.99 ± (6.6)
F2	Higuchi	0.994	1.78	37.44	93.92 ± (3.9)
F3	Higuchi	0.994	3.44	26.94	68.22 ± (5.1)
F4	Baker-Lonsdale	0.986	4.16	0.01	65.04 ± (4.8)
F5	Baker-Lonsdale	0.989	5.06	0.01	60.49 ± (2.0)
F6	Baker-Lonsdale	0.989	9.34	0.006	47.64 ± (2.3)
F7	Baker-Lonsdale	0.995	1.97	0.03	84.46 ± (1.1)
F8	Baker-Lonsdale	0.995	12.35	0.004	41.67 ± (2.8)

[a] Values are expressed as mean ($n = 3$)

Fig. 7 Optimization plot for different tested responses generated by Minitab software
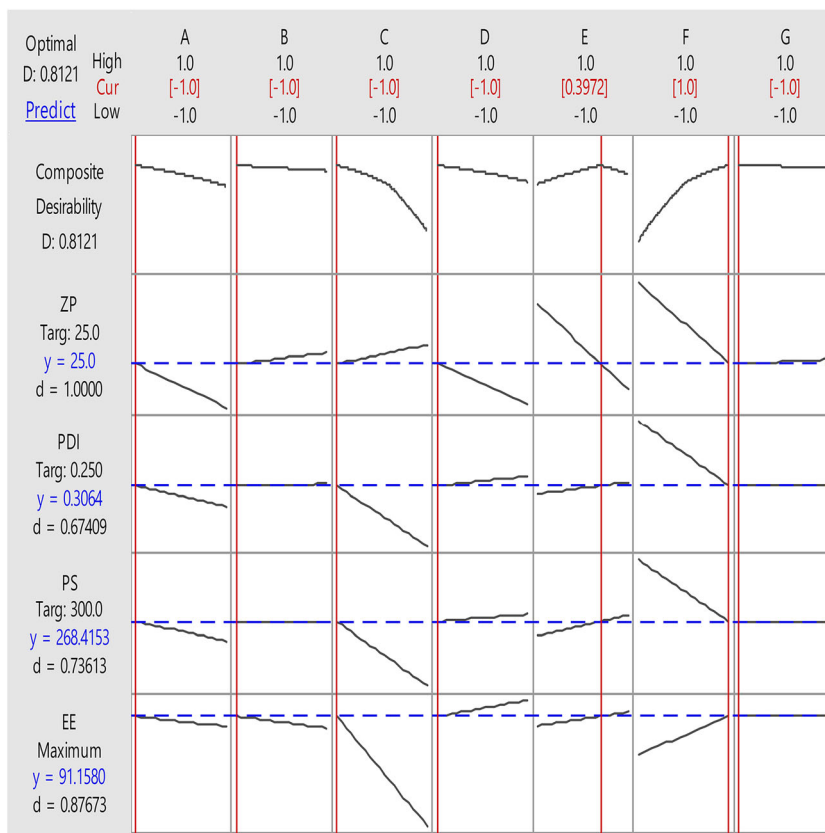
surrounding the nanocapsule dark black core in Fig. 6b) which is smooth and continuous around the oily-core.
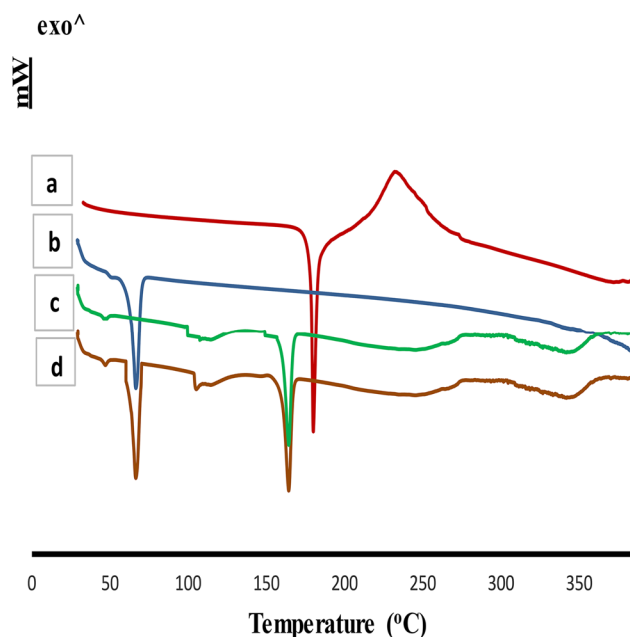
Thermal Analysis

This study revealed that the drug was converted to an amorphous form due to encapsulation inside the oily-core of the developed nanocapsules which should cause a more enhanced and rapid dissolution due to loss of crystallinity. This was confirmed by the absence of the characteristic endothermic peak of OM (180.4 °C) [30] from the DSC thermogram of freeze-dried-optimized OM-ONC while endothermic peaks of PCL (67 °C) [31] and mannitol (164.6 °C) [32] were preserved as presented in Fig. 8.

Powder X-Ray Diffraction

X-ray diffractograms which are presented in Fig. 9 show that OM diffractogram is characterized by intense diffraction peaks which are seen at 2theta values 10.56°, 11.64°, 12.54°, 14.46°, 14.85°, 16.47 °, 18.39°, 19.63°, 20.55°, 21.78°, 23.19°, and 24.63°. However, these peaks were absent or reduced in optimized freeze-dried OM-ONC diffractogram. This confirms that OM was successfully encapsulated inside the oily-core nanocapsules and it was converted to an amorphous form.

Stability Study

The results of stability study for OM-ONC (F1) are summarized in Table 5. The optimum formula showed an excellent

Fig. 8 Thermal analysis charts (DSC thermograms) of **a** pure OM, **b** PCL, **c** Mannitol, **d** freeze-dried-optimized OM-ONC
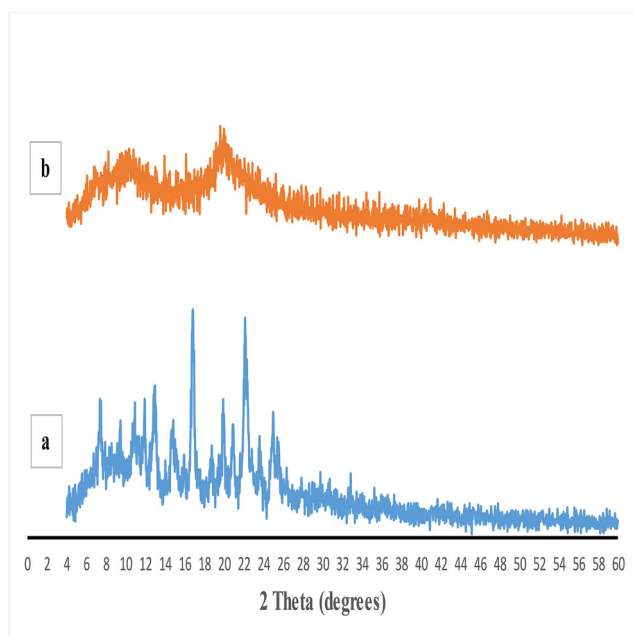
Fig. 9 X-ray diffractograms of **a** pure OM and **b** freeze-dried-optimized OM-ONC

physical stability at room temperature (25 °C) and refrigerated temperature (4 °C) for 3 months with non-significant changes to PS, PDI, and ZP. It is notable that ZP values were shifted to be more negative which enhanced the stability of the nanocapsules during storage and prevented its aggregation. EE showed also non-significant change which may be attributed to the presence of oily-core and integrity of the polymeric coat which prevented the diffusion of the solubilized drug out of the nanocapsule structure during storage.

Conclusion

The study results demonstrated that a full factorial design can be employed successfully to produce OM-ONC using nanoprecipitation technique. The prepared OM-ONC showed

Table 5 Characterization of OM-ONC (F1) during stability study for 3 months after storage at refrigerator (4 °C) and room (25 °C) temperatures

	Characteristics[a]							
	PS (nm)		PDI		ZP (mV)		%EE	
Months	4 °C	25 °C	4 °C	25 °C	4 °C	25 °C	4 °C	25 °C
0	268.6	268.60	0.28	0.28	−29.4	−29.4	94.1	94.1
1	242.6	281.00	0.32	0.26	−24.4	−31.1	93.4	91.4
2	255.9	246.80	0.25	0.24	−36.9	−34.9	92.8	89.9
3	258.7	253.33	0.30	0.28	−38.5	−35.0	91.2	88.8

[a] Values are expressed as mean ($n = 3$)

a controlled in-vitro drug release pattern and excellent physical stability. The mean values of particle size, zeta potential, polydispersity index, and entrapment efficiency indicated that the optimized formula (F1) was the one prepared using low concentration of polymer (PCL), aqueous/organic phase ratio of 1.8:1, and relatively low magnetic stirring rate. This optimized formula showed a perfect spherical morphology under TEM.

It is concluded that OM-ONC can be designed, prepared, and optimized with improved physicochemical characteristics. This optimized formula can be considered as an alternative drug delivery system for OM with enhanced biopharmaceutical properties which may increase the oral bioavailability to enhance therapeutic response and minimize side effects.

Compliance with Ethical Standards

References

1. Lee B, Kang M, Choi S, Choi B, Kim S, Lee S, et al. Solubilized formulation of olmesartan medoxomil for enhancing oral bioavailability. Arch Pharm Res. 2009;32:1629–35.
2. Thakkar H, Patel B, Thakkar S. Development and characterization of nanosuspensions of olmesartan medoxomil for bioavailability enhancement. J Pharm Bioall Sci. 2011;3(3):426–34.
3. Sharma R, Yasir M, Bhaskar S. Formulation and evaluation of paclitaxel loaded PSA-PEG nanoparticles. J Appl Pharm Sci. 2011;1:96–8.
4. Dizaj S, Vazifehasl Z, Salatin S, Adibkia K, Javadzadeh Y. Nanosizing of drugs: effect on dissolution rate. Res Pharm Sci. 2015;10(2):95–108.
5. Benita S. Microparticulate drug delivery systems: release kinetic models. In: Arshady R, editor. Microspheres, microcapsules and liposomes (the MML series). Citrus Books: London; 1998. p. 255–78.
6. Diaspro A, Krol S, Cavalleri O, Silvano D, Gliozzi A. Microscopical characterization of nanocapsules templated on ionic crystals and biological cells toward biomedical applications. IEEE Trans Nanobiosci. 2002;1(3):110–5.

7. Mora-Huertas C, Fessi H, Elaissari A. Polymer-based nanocapsules for drug delivery. Int J Pharm. 2010;385:113–42.

8. Ulery B, Nair L, Laurencin C. Biomedical applications of biodegradable polymers. J Polym Sci B Polym Phys. 2011;49:832–64.

9. Ajala T, Femi-Oyewo M, Odeku O. The effect of formulation variables on the physicochemical and antimicrobial properties of cream formulae of Phyllanthus amarus whole plant extract. West Afr J Med. 2017;28:52–60.

10. Elgindy N, Mehanna M, Mohyeldin S. Self-assembled nano-architecture liquid crystalline particles as a promising carrier for progesterone transdermal delivery. Int J Pharm. 2016;501:167–79.

11. Nasr A, Gardouh A, Ghorab M. Novel solid self-nanoemulsifying drug delivery system (S-SNEDDS) for oral delivery of olmesartan medoxomil: design, formulation, pharmacokinetic and bioavailability evaluation. Pharmaceutics. 2016;8(20):1–29.

12. Vikram K, Chander P, Varun K, Sanyog J. Nanostructured lipid carriers of olmesartan medoxomil with enhanced oral bioavailability. Colloids Surf B: Biointerfaces. 2017;154:10–20. https://doi.org/10.1016/j.colsurfb.2017.03.006.

13. Nagaraj K, Narendar D, Kishan V. Development of olmesartan medoxomil optimized nanosuspension using Box-Behnken design to improve oral bioavailability. Drug Dev Ind Pharm. 2017;43:1186–96. https://doi.org/10.1080/03639045.2017.1304955.

14. Shen J, Burgess D. In vitro dissolution testing strategies for nanoparticulate drug delivery systems: recent developments and challenges. Drug Deliv Transl Res. 2013;3:409–15. https://doi.org/10.1007/s13346-013-0129-z.

15. Hussein A. Preparation and evaluation of liquid and solid self-microemulsifying drug delivery system of mebendazole. Iraqi J Pharm Sci. 2014;23:89–100.

16. Zakia B, Suyang Z, Wenli Z, Junlin W. Formulation, development and bioavailability evaluation of a self-nanoemulsifying drug delivery system (SNEDDS) of atorvastatin calcium. Int J Pharm. 2013;29:1103–13.

17. Narendar D, Kishan V. Candesartan cilexetil loaded solid lipid nanoparticles for oral delivery: characterization, pharmacokinetic and pharmacodynamic evaluation. Drug Deliv. 2016;23:395–404.

18. Nandhakumar S, Dhanaraju M, Sundar V, Heera B. Influence of surface charge on the in vitro protein adsorption and cell cytotoxicity of paclitaxel loaded poly(e-caprolactone) nanoparticles. Bull Fac Pharm Cairo Univ. 2017;55:249–58.

19. Badri W, Miladi K, Eddabra R, Fessi H, Elaissari A. Elaboration of nanoparticles containing indomethacin: Argan oil for transdermal local and cosmetic application. J Nanomater. 2015;1:1–9.

20. Chorny M, Fishbein I, Danenberg H, Golomb G. Lipophilic drug loaded nanospheres prepared by nanoprecipitation: effect of formulation variables on size, drug recovery and release kinetics. J Control Release. 2002;83(3):389–400.

21. Rodriguez S, Allémann E, Fessi H, Doelker E. Physicochemical parameters associated with nanoparticle formation in the salting-out, emulsification diffusion and nanoprecipitation methods. Pharm Res. 2004;21(8):1428–39.

22. Asadi H, Rostamizadeh K, Salari D, Hamidi M. Preparation of biodegradable nanoparticles of tri-block PLA-PEG-PLA copolymer and determination of factors controlling the particle size using artificial neural network. J Microencapsul. 2011;28(5):406–16.

23. Honary S, Zahir F. Effect of zeta potential on the properties of nano-drug delivery systems -a review. Trop J Pharm Res. 2013;12:255–64.

24. White B, Banerjee S, O'Brien S, Turro N, Herman I. Zeta-potential measurements of surfactant-wrapped individual single-walled carbon nanotubes. J Phys Chem C. 2007;111:13684–90.

25. Kothamasu P, Kanumur H, Ravur N, Maddu C, Parasuramrajam R, Thangavel S. Nanocapsules: the weapons for novel drug delivery systems. BioImpacts. 2012;2(2):71–81.

26. Huang W, Zhang C. Tuning the size of poly(lactic-co-glycolic acid) (PLGA) nanoparticles fabricated by nanoprecipitation. Biotechnol J. 2018;13:1700203.

27. Asasutjarit R, Sorrachaitawatwong C, Tipchuwong N, Pouthai S. Effect of formulation compositions on particle size and zeta potential of diclofenac sodium-loaded chitosan nanoparticles. Int J Med Health Biomed Bioeng Pharm Eng. 2013;7(9):568–70.

28. Ajiboye A, Trivedi V, Mitchell JC. Preparation of polycaprolactone nanoparticles via supercritical carbon dioxide extraction of emulsions. Drug Deliv Transl Res. 2018;8(6):1790–6.

29. Awotwe-Otoo D, Zidan A, Rahman Z, Habib M. Evaluation of anticancer drug-loaded nanoparticle characteristics by nondestructive methodologies. AAPS PharmSciTech. 2012;13(2):611–22.

30. Arun B, Narendar D, Veerabrahma K. Development of olmesartan medoxomil lipid-based nanoparticles and nanosuspension: preparation, characterization and comparative pharmacokinetic evaluation. Artif Cells Nanomed Biotechnol. 2018;46(1):126–37.

31. Azimi B, Nourpanah P, Rabiee M, Arbab S. Poly (ε-caprolactone) fiber: an overview. J Eng Fibers Fabr. 2014;9(3):74–90.

32. Gombás Á, Szabó-Révész P, Regdon G Jr, Erős I. Study of thermal behaviour of sugar alcohols. J Therm Anal Calorim. 2003;73(2):615–21.